A band-limited uniform diffuser in transmission. II. A multilayer system

A. A. Maradudin[a], E. R. Mendez[b], T. A. Leskova[a], and I. Simonsen[c]

[a] Department of Physics and Astronomy, and Institute for Surface and Interface Science University of California, Irvine, CA 92697 U.S.A.

[b] División de Física Aplicada, Centro de Investigación Científica y de Educación Superior de Ensenada, Ensenada, Baja California 22800, México

[c] Nordic Institute for Theoretical Physics (NORDITA) Blegdamsvej 17, DK-2100 Copenhagen Ø, Denmark

ABSTRACT

In this work we consider a structure consisting of a dielectric medium characterized by a dielectric constant ϵ_1 in the region $x_3 > H$, a second dielectric medium characterized by a dielectric constant ϵ_2 in the region $\zeta(x_1) < x_3 < H$, and vacuum in the region $x_3 < \zeta(x_1)$. The surface profile function $\zeta(x_1)$ is assumed to be a single-valued function of x_1 that is differentiable and constitutes a random process. The structure is illuminated from the region $x_3 > H$ by s-polarized light whose plane of incidence is the x_1x_3-plane. By the use of the geometrical optics limit of phase perturbation theory we show how to design the surface profile function $\zeta(x_1)$ in such a way that the mean differential transmission coefficient has a prescribed form within a specified range of the angles of transmission, and vanishes outside this range. In particular, we consider the case that the incident s-polarized light is incident normally on this structure, and the mean intensity of the transmitted light is constant within a specified range of the angle of transmission, and vanishes outside it. Numerical simulation calculations show that the transmitted intensity indeed has this property.

Keywords: random surfaces, inverse problem, transmission coefficient, uniform diffuser

1. Introduction

An optical element that transmits light uniformly within a prescribed range of the angle of transmission and produces no transmission outside this range could be useful in projection systems where the desire is to illuminate a screen uniformly but not to waste light by illuminating outside the confines of the screen. Such an optical element will be called a band-limited uniform diffuser in transmission.

In a recent paper[1] a band-limited uniform diffuser was studied in the form of a dielectric film, characterized by a dielectric constant ϵ that occupied the region $-D < x_3 < \zeta(x_1)$. The region $x_3 > \zeta(x_1)$ was a vacuum, as was the region $x_3 < -D$. The surface profile function $\zeta(x_1)$ was assumed to be a single-valued function of x_1, that is differentiable, and constitutes a random process. This film was illuminated from the region $x_3 > \zeta(x_1)$ by s-polarized light, which was transmitted into the region $x_3 < -D$. By the use of methods developed earlier in Refs. 2-5 for the design of random surfaces that act as band-limited uniform diffusers in reflection, it was shown how to design the surface profile function $\zeta(x_1)$ in such a way that the mean differential transmission coefficient of the film had a prescribed form within a specified range of the angle of transmission, and vanished outside this range. This work was carried out as a reflection of the fact that the experimental demonstrations that surfaces fabricated according to the prescriptions given in Refs. 2-5 do act as band-limited uniform diffusers have been carried out for the transmission of light through dielectric films with random surfaces of this type.[3–5]

However, the structures used in the experimental studies whose results were reported in Refs. 3-5 were multilayer structures, unlike the simple film system studied theoretically in Ref. 1. Consequently, in order to make comparisons between theoretical and experimental results for the properties of band-limited uniform diffusers more meaningful, it seemed to be worthwhile to construct a theory of such diffusers on the basis of multilayer structures closer to those in Refs. 3-5. In this paper, on the basis of the geometrical optics limit of phase perturbation theory, we show how these diffusers can be designed in such a fashion that, when they are illuminated at normal incidence by s-polarized

Surface Scattering and Diffraction for Advanced Metrology, Zu-Han Gu, Alexei A. Maradudin, Editors, Proceedings of SPIE Vol. 4447 (2001) © 2001 SPIE · 0277-786X/01/$15.00

light the angular dependence of the mean intensity of the transmitted light is constant for the angle of transmission θ_t in the interval $(-\theta_m, \theta_m)$ and vanishes outside this interval. A computer simulation of the angular dependence of the mean intensity of the transmitted light confirms that the optical element designed in this way indeed possesses the properties specified for it.

2. The Transmission Amplitude

The system we consider in this work consists of a dielectric medium characterized by a dielectric constant ϵ_1 in the region $x_3 > H$; a dielectric medium characterized by a dielectric constant ϵ_2 in the region $\zeta(x_1) < x_3 < H$; and a dielectric medium characterized by a dielectric constant ϵ_3 in the region $x_3 < \zeta(x_1)$ (Fig. 1). The surface profile function $\zeta(x_1)$ is assumed to be a single-valued function of x_1 that is differentiable and constitutes a random process. In the numerical calculations carried out in this paper we will assume that the region $x_3 > H$ is glass, the region $\zeta(x_1) < x_3 < H$ is photoresist, and the region $x_3 < \zeta(x_1)$ is vacuum. The thickness of the photoresist film in the absence of the surface roughness is $H = 5\mu$m.

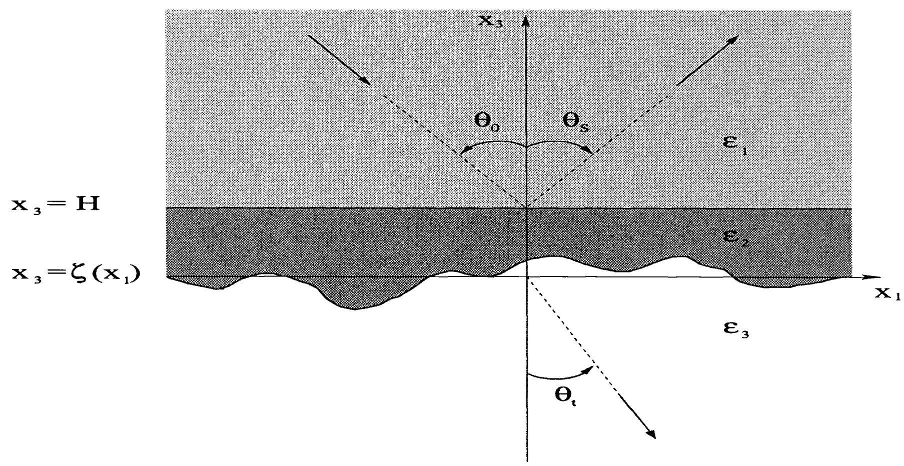

Figure 1. A sketch of the scattering system considered in the present work.

This system is illuminated from the region $x_3 > H$ by an s-polarized plane wave of frequency ω, whose plane of incidence is the x_1x_3-plane. In the numerical calculations carried out in this paper we will assume that the frequency $\omega = 2\pi c/\lambda$, where c is the speed of light in vacuum, corresponds to a wavelength $\lambda = 612.7$nm. The single nonzero component of the electric field in this system is

$$E_2(x_1, x_3|\omega) = \exp[ikx_1 - i\alpha_1(k)(x_3 - H)] + \int_{-\infty}^{\infty} \frac{dq}{2\pi} R(q|k) \exp[iqx_1 + i\alpha_1(q)(x_3 - H)] \quad (2.1)$$

in the region $x_3 > H$;

$$E_2(x_1, x_3|\omega) = \int_{-\infty}^{\infty} \frac{dq}{2\pi} \exp(iqx_1)\{B_1(q|k) \exp[-i\alpha_2(q)x_3] + B_2(q|k) \exp[i\alpha_2(q)x_3]\} \quad (2.2)$$

in the region $\zeta(x_1) < x_3 < H$;

$$E_2(x_1, x_3|\omega) = \int_{-\infty}^{\infty} \frac{dq}{2\pi} T(q|k) \exp[iqx_1 - i\alpha_3(q)x_3] \quad (2.3)$$

in the region $x_3 < \zeta(x_1)$. In these expressions the functions $\alpha_i(q)$ are defined by

$$\begin{aligned} \alpha_i(q) &= \left[\epsilon_i(\omega/c)^2 - q^2\right]^{\frac{1}{2}} & \quad |q| < \sqrt{\epsilon_i}(\omega/c) \\ &= i\left[q^2 - \epsilon_i(\omega/c)^2\right]^{\frac{1}{2}} & \quad |q| > \sqrt{\epsilon_i}(\omega/c). \end{aligned} \tag{2.4}$$

From the boundary conditions at the interface $x_3 = H$ we obtain

$$2\pi\delta(q-k) + R(q|k) = B_1(q|k)\exp[-i\alpha_2(q)H] + B_2(q|k)\exp[i\alpha_2(q)H] \tag{2.5a}$$

$$\alpha_1(q)[2\pi\delta(q-k) - R(q|k)] = \alpha_2(q)\left\{B_1(q|k)\exp[-i\alpha_2(q)H] - B_2(q|k)\exp[i\alpha_2(q)H]\right\}. \tag{2.5b}$$

Therefore,

$$B_1(q|k) = 2\pi\delta(q-k)t_{12}(k) - r_{12}(q)B_2(q|k), \tag{2.6}$$

where

$$r_{12}(q) = \frac{\alpha_1(q) - \alpha_2(q)}{\alpha_1(q) + \alpha_2(q)}\exp\{2i\alpha_2(q)H\}, \tag{2.7a}$$

$$t_{12}(q) = \frac{2\alpha_1(q)}{\alpha_1(q) + \alpha_2(q)}\exp\{i\alpha_2(q)H\}. \tag{2.7b}$$

The boundary conditions at the interface $x_3 = \zeta(x_1)$ can be written in the forms

$$\int_{-\infty}^{\infty}\frac{dq}{2\pi}\exp(iqx_1)\{B_1(q|k)\exp[-i\alpha_2(q)\zeta(x_1)] + B_2(q|k)\exp[i\alpha_2(q)\zeta(x_1)]\}$$

$$= \int_{-\infty}^{\infty}\frac{dq}{2\pi}\exp(iqx_1)T(q|k)\exp[iqx_1 - i\alpha_3(q)\zeta(x_1)] \tag{2.8a}$$

$$\int_{-\infty}^{\infty}\frac{dq}{2\pi}\exp(iqx_1)\{[\alpha_2(q) + q\zeta'(x_1)]B_1(q|k)\exp[-i\alpha_2(q)\zeta(x_1)] - [\alpha_2(q) - q\zeta'(x_1)]B_2(q|k)\exp[i\alpha_2(q)\zeta(x_1)]\}$$

$$= \int_{-\infty}^{\infty}\frac{dq}{2\pi}\exp(iqx_1)[\alpha_3(q) + q\zeta'(x_1)]T(q|k)\exp[-i\alpha_3(q)\zeta(x_1)]. \tag{2.8b}$$

If we multiply Eq. (2.8a) by $[\alpha_2(p) + p\zeta'(x_1)]\exp[-ipx_1 + i\alpha_2(p)\zeta(x_1)]$ and integrate on x_1, then multiply Eq. (2.8b) by $\exp[-ipx_1 + i\alpha_2(p)\zeta(x_1)]$ and integrate on x_1, and finally add the two resulting equations, we obtain

$$2\alpha_2(p)B_1(p|k) = (\epsilon_3 - \epsilon_2)\frac{\omega^2}{c^2}\int_{-\infty}^{\infty}\frac{dq}{2\pi}\frac{I(\alpha_3(q) - \alpha_2(p)|p-q)}{\alpha_3(q) - \alpha_2(p)}T(q|k), \tag{2.9}$$

where

$$I(\gamma|Q) = \int_{-\infty}^{\infty}dx_1\exp[-iQx_1 - i\gamma\zeta(x_1)]. \tag{2.10}$$

Similarly, if we multiply Eq. (2.8a) by $[\alpha_2(p) - p\zeta'(x_1)]\exp[-ipx_1 - i\alpha_2(p)\zeta(x_1)]$ and integrate on x_1, then multiply Eq. (2.8b) by $\exp[-ipx_1 - i\alpha_2(p)\zeta(x_1)]$ and integrate on x_1, and finally subtract the second of the resulting equations from the first, we obtain the equation

$$2\alpha_2(p)B_2(p|k) = -(\epsilon_3 - \epsilon_2)\frac{\omega^2}{c^2}\int_{-\infty}^{\infty}\frac{dq}{2\pi}\frac{I(\alpha_3(q) + \alpha_2(p)|p-q)}{\alpha_3(q) + \alpha_2(p)}T(q|k). \tag{2.11}$$

On combining (2.9) and (2.11) with Eq. (2.6) we obtain the reduced Rayleigh equation for the transmission amplitude $T(q|k)$:

$$(\epsilon_3 - \epsilon_2)\frac{\omega^2}{c^2}\int_{-\infty}^{\infty}\frac{dq}{2\pi}\left\{\frac{I(\alpha_3(q)-\alpha_2(p)|p-q)}{\alpha_3(q)-\alpha_2(p)} - r_{12}(p)\frac{I(\alpha_3(q)+\alpha_2(p)|p-q)}{\alpha_3(q)+a_2(p)}\right\}T(q|k)$$
$$= 2\pi\delta(p-k)2\alpha_2(k)t_{12}(k). \tag{2.12}$$

We solve Eq. (2.12) as an expansion in powers of the surface profile function through terms linear in $\zeta(x_1)$, with the result that

$$T(q|k) = T_0(k)[2\pi\delta(q-k) - i(\epsilon_2-\epsilon_3)\frac{\omega^2}{c^2}\frac{1}{\alpha_3(q)+\alpha_2(q)}\frac{1-r_{12}(q)}{1+r_{12}(q)r_{23}(q)}\hat{\zeta}(q-k)], \tag{2.13}$$

where

$$r_{23}(q) = \frac{\alpha_2(q)-\alpha_3(q)}{\alpha_2(q)+\alpha_3(q)}, \tag{2.14}$$

$T_0(k)$ is the Fresnel transmission amplitude in the absence of the surface roughness,

$$T_0(k) = \frac{t_{23}(k)t_{12}(k)}{1+r_{12}(k)r_{23}(k)}, \tag{2.15}$$

with

$$t_{23}(k) = \frac{2\alpha_2(k)}{\alpha_2(k)+\alpha_3(k)}, \tag{2.16}$$

and

$$\hat{\zeta}(q-k) = \int_{-\infty}^{\infty} dx_1\zeta(x_1)\exp[-i(q-k)x_1]. \tag{2.17}$$

The result given by Eq. (2.13) can be rewritten as

$$T(q|k) = T_0(k)\int_{-\infty}^{\infty} dx_1\exp[-i(q-k)x_1]\left[1 - i(\alpha_2(q)-\alpha_3(q))\frac{1-r_{12}(q)}{1+r_{12}(q)r_{23}(q)}\zeta(x_1)\right]. \tag{2.18}$$

It is more convenient to rewrite this expression identically in the form

$$T(q|k) = T_0(q|k)\int_{-\infty}^{\infty} dx_1\exp[-i(q-k)x_1][1 - i(\alpha_2(q)-\alpha_3(q))F_0(k)\zeta(x_1)], \tag{2.19}$$

where

$$T_0(q|k) = \frac{t_{12}(k)t_{23}(k)}{1-r_{12}(k)}\frac{1-r_{12}(q)}{1+r_{12}(q)r_{23}(q)}, \tag{2.20}$$

and

$$F_0(k) = \frac{1-r_{12}(k)}{1+r_{12}(k)r_{23}(k)}. \tag{2.21}$$

The phase perturbation theory for $T(q|k)$ is obtained by exponentiating the expression in brackets in the integrand of Eq. (2.19). Thus, finally, we have the result that

$$T(q|k) = T_0(q|k)\int_{-\infty}^{\infty} dx_1\exp[-i(q-k)x_1]\exp[iF(q|k)\zeta(x_1)], \tag{2.22}$$

where

$$F(q|k) = [\alpha_3(q)-\alpha_2(q)]F_0(k). \tag{2.23}$$

3. The Mean Differential Transmission Coefficient

The differential transmission coefficient $\partial T/\partial\theta_t$ is defined in such a way that $(\partial T/\partial\theta_t)d\theta_t$ is the fraction of the total time averaged incident flux that is transmitted into the angular interval $(\theta_t, \theta_t + d\theta_t)$, where θ_t is the angle of transmission (Fig. 1). The magnitude of the total time-averaged incident flux is given by

$$p_{inc} = -Re \int dx_1 \int dx_2 (S_3^c)_{inc}, \tag{3.1}$$

where S_3^c is the 3-component of the complex Poynting vector, and the minus sign compensates for the fact that the flux is in the $-x_3$-direction. In s polarization

$$S_3^c = -\frac{c}{8\pi} E_2^* H_1 = -i\frac{c^2}{8\pi\omega} E_2^* \frac{\partial E_2}{\partial x_3}. \tag{3.2}$$

Then from Eq. (2.1) we find that

$$p_{inc} = L_1 L_2 \frac{c^2}{8\pi\omega} \alpha_1(k), \tag{3.3}$$

where L_1 and L_2 are the lengths of the surface along the x_1- and x_2-axes.

The magnitude of the total time-averaged transmitted flux is given by

$$\begin{aligned} p_{tr} &= -Re \int dx_1 \int dx_2 (S_2^c)_{tr} \\ &= L_2 \frac{c^2}{8\pi\omega} \int_{-\sqrt{\epsilon_3}\frac{\omega}{c}}^{\sqrt{\epsilon_3}\frac{\omega}{c}} \frac{dq}{2\pi} \alpha_3(q) |T(q|k)|^2, \end{aligned} \tag{3.4}$$

where we have used Eq. (2.3) together with Eq. (3.2). We introduce angles of incidence and transmission, θ_0 and θ_t respectively, by (Fig. 1)

$$k = \sqrt{\epsilon_1}\frac{\omega}{c}\sin\theta_0 \qquad\qquad q = \sqrt{\epsilon_3}\frac{\omega}{c}\sin\theta_t. \tag{3.5}$$

It follows that the incident and scattered fluxes are given by

$$p_{inc} = L_1 L_2 \sqrt{\epsilon_1}\frac{c}{8\pi}\cos\theta_0 \tag{3.6}$$

$$p_{sc} = L_2 \epsilon_3 \frac{\omega}{16\pi^2} \int_{-\frac{\pi}{2}}^{\frac{\pi}{2}} d\theta_t \cos^2\theta_t |T(q|k)|^2. \tag{3.7}$$

The differential transmission coefficient by definition is then given by

$$\frac{\partial T}{\partial\theta_t} = \frac{1}{L_1}\frac{\epsilon_3}{\sqrt{\epsilon_1}}\frac{\omega}{2\pi c}\frac{\cos^2\theta_t}{\cos\theta_0}|T(q|k)|^2. \tag{3.8}$$

Since we are studying transmission through a random surface, it is the mean differential reflection coefficient that is of interest to us. It is given by

$$\left\langle \frac{\partial T}{\partial\theta_t} \right\rangle = \frac{1}{L_1}\frac{\epsilon_3}{\sqrt{\epsilon_1}}\frac{\omega}{2\pi c}\frac{\cos^2\theta_t}{\cos\theta_0}\langle |T(q|k)|^2 \rangle, \tag{3.9}$$

where the angle brackets denote an average over the ensemble of realizations of the surface profile function $\zeta(x_1)$. On combining Eqs. (2.22) and (3.9) we find that in phase perturbation theory

$$\begin{aligned} \left\langle \frac{\partial T}{\partial\theta_t} \right\rangle &= \frac{1}{L_1}\frac{\epsilon_3}{\sqrt{\epsilon_1}}\frac{\omega}{2\pi c}\frac{\cos^2\theta_t}{\cos\theta_0}|T_0(q|k)|^2 \\ &\times \int_{-\infty}^{\infty} dx_1 \int_{-\infty}^{\infty} dx_1' \exp[-i(q-k)(x_1 - x_1')] \langle \exp\{i[F(q|k)\zeta(x_1) - F^*(q|k)\zeta(x_1')]\}\rangle. \end{aligned} \tag{3.10}$$

In order to pass to the geometrical optics limit of phase perturbation theory, we have to work in a parameter range where the coefficients of $\zeta(x_1)$ and $\zeta(x_1')$ in the exponent in the integrand in Eq. (3.10) are the same and real. This requires that the inequality

$$|F_2(q|k)| \ll |F_1(q|k)|, \tag{3.11}$$

where $F_1(q|k) = ReF(q|k)$ and $F_2(q|k) = ImF(q|k)$, be satisfied. As long as the range of scattering angles does not reach the critical angle for total internal reflection at the photoresist/vacuum interface, $F_1(q|k) = (\alpha_3(q) - \alpha_2(q))ReF_0(k)$ and $F_2(q|k) = (\alpha_3(q) - \alpha_2(q))ImF_0(k)$, and we can always choose the thickness of the photoresist film to minimize $ImF_0(k)$. For the values of the parameters to be used in our numerical calculations $|F_2(q|k)| \cong \frac{1}{22}|F_1(q|k)|$. Consequently, we will neglect $F_2(q|k)$ in what follows with the result that the expression (3.10) for $\langle\partial T/\partial\theta_t\rangle$ now takes the form

$$\left\langle\frac{\partial T}{\partial\theta_t}\right\rangle = \frac{1}{L_1}\frac{\epsilon_3}{\sqrt{\epsilon_1}}\frac{\omega}{2\pi c}\frac{\cos^2\theta_t}{\cos\theta_0}|T_0(q|k)|^2\int_{-\infty}^{\infty}dx_1\int_{-\infty}^{\infty}dx_1'\exp[-i(q-k)(x_1')]\langle\exp[iF_1(q|k)(\zeta(x_1)-\zeta(x_1'))]\rangle. \tag{3.12}$$

We now make the change of variable $x_1' = x_1 + u$, and obtain

$$\left\langle\frac{\partial T}{\partial\theta_t}\right\rangle = \frac{1}{L_1}\frac{\epsilon_3}{\sqrt{\epsilon_1}}\frac{\omega}{2\pi c}\frac{\cos^2\theta_t}{\cos\theta_0}|T_0(q|k)|^2\int_{-\infty}^{\infty}dx_1\int_{-\infty}^{\infty}du\exp[i(q-k)u]\langle\exp[iF_1(q|k)(\zeta(x_1)-\zeta(x_1+u))]\rangle. \tag{3.13}$$

To obtain the geometrical optics limit of this expression, we expand the difference $\zeta(x_1) - \zeta(x_1+u)$ in powers of u, and retain only the term linear in u. Thus, we have in this limit

$$\left\langle\frac{\partial T}{\partial\theta_t}\right\rangle = \frac{1}{L_1}\frac{\epsilon_3}{\sqrt{\epsilon_1}}\frac{\omega}{2\pi c}\frac{\cos^2\theta_t}{\cos\theta_0}|T_0(q|k)|^2\int_{-\infty}^{\infty}dx_1\int_{-\infty}^{\infty}du\exp[i(q-k)u]\langle\exp[-iF_1(q|k)u\zeta'(x_1)]\rangle. \tag{3.14}$$

In what follows we specialize to the case of normal incidence: $\theta_0 = 0$, so that $k = 0$. In this case Eq. (3.14) becomes

$$\left\langle\frac{\partial T}{\partial\theta_t}\right\rangle = \frac{1}{L_1}\frac{\epsilon_3}{\sqrt{\epsilon_1}}\frac{\omega}{2\pi c}\cos^2\theta_t|T_0(q|0)|^2\int_{-\infty}^{\infty}dx_1\int_{-\infty}^{\infty}du\exp(iqu)\langle\exp[-iF_1(q|0)u\zeta'(x_1)]\rangle. \tag{3.15}$$

This expression is the starting point for the determination of a surface profile function $\zeta(x_1)$ that yields a specified form for $\langle\partial T/\partial\theta_t\rangle$.

4. The Surface Profile Function $\zeta(x_1)$

We assume that the surface profile function $\zeta(x_1)$ is written in the form [2]

$$\zeta(x_1) = \sum_{t=-\infty}^{\infty} c_\ell s(x_1 - \ell 2b), \tag{4.1}$$

where the $\{c_\ell\}$ are independent, positive, random deviates, b is a characteristic length, and the function $s(x_1)$ is defined by

$$s(x_1) = \begin{cases} 0 & x_1 < -(m+1)b \\ -(m+1)bh - hx_1 & -(m+1)b < x_1 < -mb \\ -bh & -mb < x_1 < mb \\ -(m+1)bh + hx_1 & mb < x_1 < (m+1)b \\ 0 & (m+1)b < x_1, \end{cases} \tag{4.2}$$

where m is a positive integer. Due to the positivity of the coefficient c_ℓ, its probability density function (pdf) $f(\gamma) = \langle\delta(\gamma - c_\ell)\rangle$ is nonzero only for $\gamma > 0$.

It has been shown [2] that for the random surfaces defined by Eqs. (4.1) and (4.2),

$$\int_{-\infty}^{\infty} dx_1 \int_{-\infty}^{\infty} du \exp(iqu)\langle\exp[-iF_1(q|0)u\zeta'(x_1)]\rangle = \frac{\pi L_1}{|F_1(q|0)|h}\left[f\left(\frac{q}{|F_1(q|0)|h}\right) + f\left(\frac{-q}{|F_1(q|0)|h}\right)\right]. \tag{4.3}$$

On combining Eqs. (3.15) and (4.3) we find that the mean differential transmission coefficient is given in terms of the pdf of c_ℓ by

$$\left\langle\frac{\partial T}{\partial\theta_t}\right\rangle = \frac{\epsilon_3}{\sqrt{\epsilon_1}}\frac{\omega}{2c}\cos^2\theta_t|T_0(q|0)|^2\frac{1}{|F_1(q|0)|h}\left[f\left(\frac{q}{|F_1(q|0)|h}\right) + f\left(\frac{-q}{|F_1(q|0)|h}\right)\right]. \tag{4.4}$$

We now make the change of variable $(q/|F_1(q|0)|h) = \gamma$, so that

$$\gamma h = \frac{q}{|F_1(q|0)|} = \frac{\sqrt{\epsilon_3}(\omega/c)\sin\theta_t}{|F_1(\sqrt{\epsilon_3}(\omega/c)\sin\theta_t|0)|}. \tag{4.5}$$

We need to invert this expression to obtain $\sin\theta_t$ and $\cos\theta_t$ as functions of γ. Equation (4.5) can be quite easily inverted with the result

$$\tan\theta_t = \frac{\gamma h|ReF_0(0)|}{\epsilon_3 + \gamma^2h^2|ReF_0(0)|^2(\epsilon_2 - \epsilon_3)}\left[\epsilon_3 - \sqrt{\epsilon_2\epsilon_3 - \gamma^2h^2|ReF_0(0)|^2(\epsilon_2 - \epsilon_3)^2}\right], \tag{4.6}$$

from which $\sin\theta_t$ and $\cos\theta_t$ can be obtained. On inverting Eq. (4.4) with the aid of these results we find that

$$f(\gamma) + f(-\gamma) = 2h\frac{\sqrt{\epsilon_1}}{\sqrt{\epsilon_3}|T_0(\sqrt{\epsilon_3}(\omega/c)s(\gamma h)|0)|^2}\frac{s(\gamma h)}{\gamma hc^2(\gamma h)}\left\langle\frac{\partial T}{\partial\theta_t}\right\rangle(\gamma), \tag{4.7}$$

where $\sin\theta_t = s(\gamma h)$ and $\cos\theta_t = c(\gamma h) = [1 - s^2(\gamma h)]^{\frac{1}{2}}$.

Thus, if we wish to design a surface for which $\langle\partial T/\partial\theta_t\rangle$ has the form

$$\left\langle\frac{\partial T}{\partial\theta_t}\right\rangle = A\theta(\theta_m - |\theta_t|), \tag{4.8}$$

where A is a constant and $\theta(x)$ is the Heaviside unit step function, we can use the fact that θ_t is a single-valued function of γh that increases monotonically with increasing γh, to rewrite Eq. (4.8) as

$$\left\langle\frac{\partial T}{\partial\theta_t}\right\rangle(\gamma) = A\theta(\gamma_m - |\gamma|), \tag{4.9}$$

where

$$\gamma_m = \frac{1}{h}\frac{\sqrt{\epsilon_3}(\omega/c)\sin\theta_m}{|F_1(\sqrt{\epsilon_3}(\omega/c)\sin\theta_m|0)|}. \tag{4.10}$$

If we substitute Eq. (4.9) into Eq. (4.7) and assume that γ is positive, we obtain finally that the pdf of c_ℓ is given by

$$f(\gamma) = 2h\frac{\sqrt{\epsilon_1}}{\sqrt{\epsilon_3}|T_0(\sqrt{\epsilon_3}(\omega/c)s(\gamma h)|0)|^2}\frac{s(\gamma h)}{\gamma hc^2(\gamma h)}A\theta(\gamma_m - \gamma)\theta(\gamma). \tag{4.11}$$

The constant A is then obtained from the normalization condition

$$2h\frac{\sqrt{\epsilon_1}}{\sqrt{\epsilon_3}}A\int_0^{\gamma_m} d\gamma\frac{s(\gamma h)}{\gamma hc^2(\gamma h)|T_0(\sqrt{\epsilon_3}(\omega/c)s(\gamma h)|0)|^2} = 1 \tag{4.12}$$

or

$$A\frac{2\sqrt{\epsilon_1}}{\sqrt{\epsilon_3}}\int\limits_0^{h\gamma_m} dx \frac{s(x)}{xc^2(x)|T_0(\sqrt{\epsilon_3}(\omega/c)s(x)|0)|^2} = 1. \tag{4.13}$$

If we note from Eq. (4.10) that

$$h\gamma_m = \frac{\sqrt{\epsilon_3}(\omega/c)\sin\theta_m}{|F_1(\sqrt{\epsilon_3}(\omega/c)\sin\theta_m|0)|}, \tag{4.14}$$

we find that the constant A is independent of the parameter h. For the parameters used to define the surface, we find that $f(\gamma)$ is nearly a constant function of γ, but decreases slowly and monotonically over the range $0 \leq \gamma \leq \gamma_m$.

5. Results

An ensemble of one-dimensional random surfaces was generated on the basis of the preceding results. For each member of the ensemble a sequence of the coefficients $\{c_\ell\}$ was obtained by the rejection method [6], and the surface profile function generated by the use of Eqs. (4.1) and (4.2). The values of the parameters m, b, h entering Eq. (4.2) were chosen to be $m = 1, b = 55\mu m$, $h = 0.01$, while $\theta_m = 7°$. The film structure depicted in Fig. 1 was characterized by the values $H = 5\mu m$, and $\epsilon_1 = 2.25$ (glass), $\epsilon_2 = 2.69$ (photoresist), $\epsilon_3 = 1$ (vacuum).

This system was illuminated at normal incidence by an s-polarized plane wave of wavelength $\lambda = 612.7nm$ (in vacuum). The mean differential transmission coefficient was then calculated by the use of a rigorous numerical approach based on the use of Green's second integral identity in the plane.[7] The length of the x_1-axis covered by the random surface was $L = 60.6\mu m = 98.9\lambda$, and the sampling length was $\Delta x \simeq \lambda/10$. The results from $N_p = 2972$ realizations of the random surface were averaged in obtaining the mean differential transmission coefficient. We note that the surfaces studied were sufficiently rough that the contribution to the mean differential transmission coefficient from the light transmitted coherently was negligible compared to the contribution from the light transmitted incoherently. Consequently, it sufficed to calculate only the mean differential transmission coefficient.

The surface profiles generated according to Eq. (4.1) do not have a vanishing mean. Therefore, for each realization of the surface used in the numerical simulation calculations, its mean was adjusted to zero in order to have a well-defined mean film thickness H, independent of the parameters used to generate the surface profile function.

The result for the mean differential transmission coefficient is plotted in Fig. 2a as a function of the angle of transmission θ_t. It is seen to be very well band-limited, being nonzero only for $-7° < \theta_t < 7°$. It is also reasonably uniform within this interval of angles of transmission.

It should be mentioned that in order to obtain the numerical result presented in Fig. 2a we had to shift the lower limit of $f(\gamma)$ slightly away from zero, $\gamma \to \gamma - \epsilon$, $\epsilon = 0.1$, in order to avoid a small specular peak that is due to the tails of the two distributions in Eq. (4.4) caused by diffraction effects. This procedure has been described in detail in Ref. 2, and the arguments for doing so will not be repeated here.

The results obtained in Ref. 7 enables us to calculate the mean differential reflection coefficient, $\langle \partial R_s/\partial\theta_s \rangle$, from the structure depicted in Fig. 1. In Fig. 2b we present a plot of $\langle \partial R_s/\partial\theta_s \rangle$ as a function of the scattering angle θ_s. The experimental, material, and computational parameters assumed in obtaining this result are exactly the same as the ones assumed in obtaining the result plotted in Fig. 2a. It is seen to be band-limited, being nonzero only for $|\theta_s|$ smaller then approximately 23°, and reasonably constant within this interval. An argument based on the application of Snell's law at each interface yields the following relation between the maximum angle defining the angular region within which the mean differential reflection coefficient is nonzero and θ_m:

$$\sin\theta_s = \left(\frac{\epsilon_2}{\epsilon_1}\right)^{\frac{1}{2}} \frac{2\sin\theta_m(\sqrt{\epsilon_2} - \cos\theta_m)}{\epsilon_2 + 1 - 2\sqrt{\epsilon_2}\cos\theta_m}. \tag{5.1}$$

For a value of $\theta_m = 7°$, this expression yields $\theta_s = 23.4°$, which agrees well with the result depicted in Fig. 2b. This angle is indicated by vertical dashed lines in this figure. The dip at $\theta_s = 0°$ is caused by the shift of $f(\gamma)$, and could be reduced or eliminated by varying the shift parameter ϵ. In view of the fact that the surface profile function $\zeta(x_1)$ was not designed to produce a band-limited uniform diffuser in reflection, but only in transmission, the result for $\langle \partial R/\partial\theta_s \rangle$ depicted in Fig. 2b is felt to be quite satisfactory.

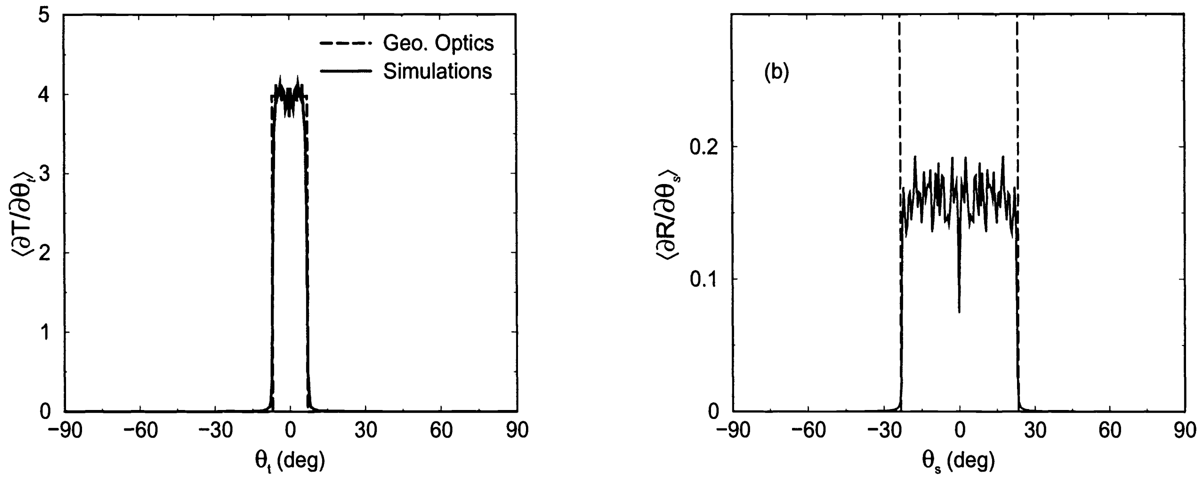

Figure 2. (a) The mean differential transmission coefficient for s-polarized (plane wave) light of wavelength $\lambda = 612.7nm$ (in vacuum) incident normally on the structure depicted in Fig. 1. The dielectric constants of the layers consituting this structure are $\epsilon_1 = 2.25, \epsilon_2 = 2.69, \epsilon_3 = 1$, and the mean thickness of the film is $H = 5\mu m$. The solid curve is the result of rigorous Monte Carlo simulations, while the dashed curve is the result given by Eqs. (4.8) and (4.12). The length of the surface used in the simulations was $L_1 = 60.6\mu m = 98.9\lambda$, and the number of surface realizations over which $\partial T/\partial\theta_t$, was averaged was $N_p = 2972$. The number of sampling points used was $N = 1000\,(\Delta x \simeq \lambda/10)$. The random surface was characterized by the parameters $m = 1, b = 55\mu m, h = 0.01, \theta_m = 7°$. (b) The same as (a), but now showing the rigorous Monte Carlo simulations for the mean differential reflection coefficient. The vertical dashed lines are the predictions obtained from Eq. (5.1).

6. Conclusions

In this paper we have derived the reduced Rayleigh equation, Eq. (2.12), for the transmission amplitude $T(q|k)$ in the case that the structure depicted in Fig. 1 is illuminated from the region $x_3 > H$ by s-polarized light whose plane of incidence is normal to the generators of the random surface $x_3 = \zeta(x_1)$. The phase perturbation theory solution of this equation, Eq. (2.22), has been obtained to the lowest nonzero order in the surface profile function $\zeta(x_1)$. The use of this solution in the expression (3.9) for the mean differential transmission coefficient enabled this coefficient to be calculated in the geometrical optics limit of phase perturbation theory, Eq. (3.14). These three results by themselves could be useful in future studies of the transmission of light through the multilayer structure presented in Fig. 1.

The result for the mean differential transmission coefficient in the geometrical optics limit of phase perturbation theory has then been used to design the random surface $x_3 = \zeta(x_1)$ in Fig. 1 in such a way that the resulting structure acts as a band-limited uniform diffuser. That is, the angular dependence of the intensity of the transmitted light is constant within a specified range of the angle of transmission, and vanishes outside that region. The results of numerical simulations of the transmission of s-polarized light through the structure in Fig. 1 whose random surface has been defined in this way show that it indeed acts as a band-limited diffuser. The transmitted intensity, although reasonably uniform, is not quite as uniform as the input mean differential transmission coefficient given by Eq. (4.8). We believe that this feature of our result can be improved by using more realizations of the random surface in our computer simulations, and by using a larger value of the length b, and hence of the length of the random surface L_1, in these simulations. However, the computational time for obtaining $\langle\partial T/\partial\theta_s\rangle$ when both of these steps are implemented is increased very significantly over the length of what are already lengthy calculations. We have therefore not implemented them. We have also shown that the very same structure and the very same random surface, also acts as a band-limited uniform diffuser in reflection, when s-polarized light is incident normally on it.

The angular interval within which the intensity of the scattered light is nonzero is wider than it is in transmission, and a relation between the angular width of the mean differential reflection coefficient and that of the mean differential transmission coefficient has been presented. Thus, the results obtained in this paper show that the approach used in our earlier papers to generate one-dimensional random surfaces that act as one-dimensional band-limited uniform diffusers in reflection can be applied to solve the same problem in transmission as well.

ACKNOWLEDGEMENTS

The research of T. A. L. and A. A. M. was supported in part by Army Research Office Grant DAAG 19-99-1-0321. The research of E.R.M. was supported in part by CONACYT Grant 32254-E.

REFERENCES

1. T. A. Leskova, A. A. Maradudin, E. R. Méndez, and I. Simonsen, "A band-limited uniform diffuser in transmission," SPIE **4100**, 113–123 (2000).
2. E. R. Méndez, G. Martinez-Niconoff, A. A. Maradudin, and T. A. Leskova, "Design and synthesis of random uniform diffusers," SPIE **3426**, 2–14 (1998).
3. T. A. Leskova, A. A. Maradudin, E. R. Méndez, and A. V. Shchegrov, "The design and fabrication of one-dimensional random surfaces with specified scattering properties," *Physics of the Solid State* **41**, 835–841 (1999).
4. A. A. Maradudin, "Multiple-scattering phenomena in the scattering of light from randomly rough surfaces," *phys. stat. solidi (a)* **175**, 241–252 (1999).
5. E. I. Chaikina, E. E. García-Guerrero, Z.-H. Gu, T. A. Leskova, A. A. Maradudin, E. R. Méndez, and A. V. Shchegrov, "Multiple-scattering phenomena in the scattering of light from randomly rough surfaces," in *Frontiers of Laser Physics and Quantum Optics*, eds. Z. Xu. S. Xie, S. Y. Zhu, and M. O. Scully (Springer-Verlag, New York, 2000), pp. 225–259.
6. W. H. Press, S. A. Teukolsky, W. T. Vetterling, and B. P. Flannery, *Numerical Recipes in Fortran, 2nd ed.* (Cambridge University Press, New York, 1992), pp. 281–182.
7. I. Simonsen, T. A. Leskova, A. A. Maradudin, and O. Hunderi, "Wavelength dependence of the light scattered from a dielectric film deposited on a metal substrate," SPIE **4100**, 65-77 (2000).